

1 **One-million-year-old DNA sheds light on the genomic history of
2 mammoths**

3
4 Tom van der Valk^{1,2,3*}, Patricia Pečnerová^{2,4,5*}, David Díez-del-Molino^{1,2,4*}, Anders Bergström⁶,
5 Jonas Oppenheimer⁷, Stefanie Hartmann⁸, Georgios Xenikoudakis⁸, Jessica A. Thomas⁸,
6 Marianne Dehasque^{1,2,4}, Ekin Sağlıcan⁹, Fatma Rabia Fidan⁹, Ian Barnes¹⁰, Shanlin Liu¹¹,
7 Mehmet Somel⁹, Peter D. Heintzman¹², Pavel Nikolskiy¹³, Beth Shapiro^{14,15}, Pontus Skoglund⁶,
8 Michael Hofreiter⁸, Adrian M. Lister¹⁰, Anders Götherström^{1,16#}, Love Dalén^{1,2,4#}

9
10 1. Centre for Palaeogenetics, Svante Arrhenius väg 20C, SE-106 91 Stockholm, Sweden
11 2. Department of Bioinformatics and Genetics, Swedish Museum of Natural History, Stockholm, Sweden
12 3. Department of Cell and Molecular Biology, National Bioinformatics Infrastructure Sweden, Science for Life
13 Laboratory, Uppsala University, Uppsala, Sweden
14 4. Department of Zoology, Stockholm University, SE-106 91 Stockholm, Sweden
15 5. Section for Computational and RNA Biology, Department of Biology, University of Copenhagen, DK-2200
16 Copenhagen, Denmark
17 6. The Francis Crick Institute, London NW1 1AT, UK
18 7. Department of Biomolecular Engineering, University of California Santa Cruz, Santa Cruz, CA, USA
19 8. Institute for Biochemistry and Biology, University of Potsdam, 14476 Potsdam, Germany
20 9. Department of Biological Sciences, Middle East Technical University, Ankara, Turkey
21 10. Department of Earth Sciences, Natural History Museum, London SW7 5BD, UK.
22 11. College of Plant Protection, China Agricultural University, Beijing 100193, China
23 12. The Arctic University Museum of Norway, UiT - The Arctic University of Norway, 9037 Tromsø, Norway
24 13. Geological Institute, Russian Academy of Sciences, Moscow, Russia
25 14. Department of Ecology and Evolutionary Biology, University of California Santa Cruz, Santa Cruz, CA, USA
26 15. Howard Hughes Medical Institute, University of California Santa Cruz, Santa Cruz, CA 96054 USA
27 16. Department of Archaeology and Classical Studies, Stockholm University, SE-106 91 Stockholm, Sweden

28
29 *) These authors contributed equally: Tom van der Valk, Patrícia Pečnerová, David Díez-del-Molino
30 #) These authors jointly supervised this work: Anders Götherström and Love Dalén

31 Correspondence: tom.vandervalk@scilifelab.se, love.dalen@nrm.se

33 **Abstract**

34 Temporal genomic data hold great potential for studying evolutionary processes, including
35 speciation. However, sampling across speciation events would in many cases require genomic
36 time series that stretch well into the Early Pleistocene (>1 million years). Although theoretical
37 models suggest that DNA should survive on this timescale¹, the oldest genomic data recovered
38 so far is from a 560-780 ka old horse specimen². Here we report the recovery of genome-wide
39 data from three Early and Middle Pleistocene mammoth specimens, two of which are more than
40 one million years old. We find that two distinct mammoth lineages were present in eastern
41 Siberia during the Early Pleistocene. One of these gave rise to the woolly mammoth, whereas
42 the other represents a previously unrecognised lineage that was ancestral to the first
43 mammoths to colonise North America. Our analyses reveal that the North American Columbian
44 mammoth traces its ancestry to a Middle Pleistocene hybridisation between these two lineages,
45 with roughly equal admixture proportions. Finally, we show that the majority of protein-coding
46 changes associated with cold adaptation in woolly mammoths were present already a million
47 years ago. These findings highlight the potential of deep time palaeogenomics to expand our
48 understanding of speciation and long-term adaptive evolution.

49 **Main**

50 The recovery of genomic data from specimens that are many thousands of years old has
51 improved our understanding of prehistoric population dynamics, ancient introgression events,
52 and the demography of extinct species³⁻⁵. However, some evolutionary processes occur over
53 time scales that have often been considered beyond the temporal limits of ancient DNA
54 research. For example, many present-day mammal and bird species originated during the Early
55 and Middle Pleistocene^{6,7}. Palaeogenomic investigations of their speciation process would thus
56 require recovery of ancient DNA from specimens that are at least several hundreds of
57 thousands of years (ka) old.

58 Mammoths (*Mammuthus* sp.) appeared in Africa approximately 5 million years ago (Ma) and
59 subsequently colonised much of the Northern Hemisphere^{8,9}. During the Pleistocene (2.6 Ma -
60 11.7 ka), the mammoth lineage underwent evolutionary changes that resulted in early species
61 known as the southern (*Mammuthus meridionalis*) and steppe (*M. trogontherii*) mammoths,
62 which later gave rise to the Columbian (*M. columbi*) and woolly (*M. primigenius*) mammoths¹⁰.
63 Although the exact relationships among these taxa are uncertain, the prevailing view is that the
64 Columbian mammoth evolved during an early colonisation of North America c. 1.5 Ma, whereas
65 the woolly mammoth first appeared in northeastern Siberia c. 0.7 Ma^{8,10}. *M. trogontherii*-like
66 mammoths, considered to be a single species, inhabited Eurasia since at least c. 1.7 Ma, with
67 the last populations going extinct in Europe at c. 0.2 Ma⁸.

68 To investigate the origin and evolution of woolly and Columbian mammoths, we recovered
69 genomic data from three northeastern Siberian mammoth molars dated to the Early and Middle
70 Pleistocene (Fig. 1a; Extended Data Fig. 1; Extended Data Fig. 2). These molars originate from
71 the well-documented and fossiliferous Olyorian Suite of northeastern Siberia¹¹, which has been
72 dated using rodent biostratigraphy tied to the global sequence of palaeomagnetic reversals as
73 well as to correlated faunas with absolute dating from eastern Beringia (Extended Data Fig. 2,
74 Supplementary Section 1). One of the specimens (Krestovka) is morphologically similar to the

75 steppe mammoth, a species originally defined from the European Middle Pleistocene
76 (Supplementary Section 1), and was collected from Lower Olyorian deposits that have been
77 dated to 1.2 - 1.1 Ma. The second specimen (Adycha), which is also of *trogontherii*-like
78 morphology (Supplementary Section 1), is of less certain age within the Olyorian (1.2 - 0.5 Ma).
79 However, the morphology of the Adycha specimen (Extended data Fig. 1) strongly suggests that
80 it dates to the Early Olyorian, 1.2 - 1.0 Ma. The third specimen (Chukochya) has a morphology
81 consistent with an early form of woolly mammoth (Extended data Fig. 1) and was discovered in
82 a section where only Upper Olyorian deposits are exposed, implying an approximate age of 0.8
83 - 0.5 Ma (Supplementary Section 1).

84 We extracted DNA from the three molars using methods designed to recover highly degraded
85 DNA fragments^{12,13}, converted the extracts into libraries¹⁴, and sequenced these on Illumina
86 platforms (Supplementary Section 2; Supplementary Table 1). The reads were merged and
87 mapped against the African savannah elephant (*Loxodonta africana*) genome (LoxAfr4)¹⁵ and
88 an Asian elephant (*Elephas maximus*) mitochondrial genome¹⁶. We found that the DNA
89 recovered from the Early and Middle Pleistocene specimens was considerably more fragmented
90 and had higher levels of cytosine deamination than DNA from Late Pleistocene permafrost
91 samples (Extended Data Figs. 3, 4, Supplementary Section 4). To circumvent this, we used
92 conservative filters and an iterative approach designed to minimise spurious mappings of short
93 reads (Supplementary Section 5). This approach allowed us to recover complete (>37X
94 coverage) mitogenomes from all three specimens, and 49, 884, and 3,671 million base pairs of
95 nuclear genomic data for Krestovka, Adycha, and Chukochya, respectively (Supplementary
96 Table 3).

97 **DNA-based age estimates**

98 To estimate specimen ages using mitogenome data, we conducted a Bayesian molecular clock
99 analysis, calibrated using samples with finite radiocarbon dates (tip calibration) and a log-normal
100 prior assuming a 5.3 Ma genomic divergence between the African elephant and mammoth
101 lineages¹⁵ (root calibration). This provided specimen age estimates of 1.65 Ma (95% HPD: 2.08-
102 1.25 Ma), 1.34 (1.69-1.06 Ma), and 0.87 Ma (1.07-0.68 Ma) for Krestovka, Adycha, and
103 Chukochya, respectively (Fig. 1c,e). We also used the autosomal genomic data to investigate
104 the age of the higher-coverage Adycha (0.3X) and Chukochya (1.4X) specimens by estimating
105 the number of derived changes since their common ancestor with the African elephant
106 (Supplementary Section 6). We used an approach based on the accumulation of derived
107 variants over time¹⁷, assuming a constant mutation rate. This resulted in inferred ages of 1.28
108 Ma (95% CI 1.64-0.92 Ma) for the Adycha specimen and 0.62 Ma (95% CI 1.00-0.24 Ma) for the
109 Chukochya specimen (Fig. 1d). Although we caution that this analysis is based on low-coverage
110 data and the confidence intervals are wide, these estimates are similar to those obtained from
111 the mitochondrial data.

112 The DNA-based age estimates for the Chukochya and Adycha specimens are consistent with
113 the independently derived geological age inferences from biostratigraphy and
114 palaeomagnetism, whereas molecular clock dating of the Krestovka specimen suggests an
115 older age compared to that obtained from biostratigraphy. This could mean that the Krestovka
116 specimen had been reworked from an older geological deposit or that the mitochondrial clock

117 rate has been underestimated. However, the confidence intervals of the genetic and geological
118 age estimates of the Krestovka specimen are separated by only 0.05 Ma, and all estimates
119 support an age greater than one million years.

120 **A genetically divergent mammoth lineage**

121 A phylogeny based on autosomal data shows that the three Early/Middle Pleistocene samples
122 fall outside the diversity of all Late Pleistocene Eurasian mammoth genomes (Fig. 1b), including
123 two woolly mammoth genomes from Europe (Scotland; 48 ka) and Siberia (Kanchalan; 24 ka)
124 generated as part of this study. The phylogenetic positions of Adycha and Chukochya are
125 consistent with these genomes being from a population directly ancestral to all Late Pleistocene
126 woolly mammoths, whereas the Krestovka mammoth genome diverged prior to the split
127 between Columbian and woolly mammoth genomes (Fig. 1b). Similarly, Bayesian reconstruction
128 of a mitogenome phylogeny that included 168 Late Pleistocene mammoth specimens^{18,19} places
129 the Early Pleistocene Krestovka and Adycha specimens as basal to all previously published
130 mammoth mitogenomes, whereas the Middle Pleistocene Chukochya mitogenome is basal to
131 one of the three clades previously described for Late Pleistocene woolly mammoths²⁰ (Fig. 1c).

132 Estimates of sequence divergence times based on both genome-wide and mitochondrial data
133 indicate a deep split between Krestovka and all other mammoths analysed in this study. We
134 estimate that the Krestovka mitogenome diverged from all other mammoth mitogenomes
135 between 2.66 and 1.78 Ma (95% HPD, Fig. 1c). We obtained a similar divergence time estimate
136 (95% CI 2.65 - 1.96 Ma) from the autosomal data, but caution that this analysis is based on
137 limited genomic data (Supplementary Section 7). Moreover, estimates of relative divergence
138 using $F(A|B)$ statistics⁴ show that the Krestovka nuclear genome carries fewer derived alleles
139 than any other mammoth genome at sites where the high-coverage woolly mammoth genomes
140 are heterozygous, further supporting that it diverged after the split with Asian elephant but
141 before any of the other mammoth genomes analysed here (Extended Data Fig. 5,
142 Supplementary Section 8).

143 Overall, these analyses suggest that two evolutionary lineages (*i.e.* two isolated populations
144 persisting through time) of mammoths inhabited eastern Siberia during the latter stages of the
145 Early Pleistocene. One of these lineages, which is represented by the Krestovka specimen,
146 diverged from other mammoths prior to the first appearance of mammoths in North America.
147 The second lineage comprises the Adycha specimen along with all Middle and Late Pleistocene
148 woolly mammoths.

149 **Origin of the Columbian mammoth**

150 Intriguingly, several lines of evidence suggest that, compared to all other mammoths, the
151 Columbian mammoth derives a much higher proportion of its ancestry from the lineage
152 represented by the Krestovka mammoth. Analyses using D-statistics⁴ revealed a strong signal
153 of excess derived allele sharing between the Columbian mammoth and Krestovka (Fig. 2a,
154 Supplementary Section 8). This is at odds with the average phylogenetic position of Krestovka
155 being basal to all other mammoth genomes, since under a scenario without subsequent
156 admixture the D-statistic would not deviate from zero. We further investigated this pattern using

157 TreeMix²¹. Without modelling migration (admixture) events, none of the models fit the data
158 (residuals >10x SE). Instead, we observed a good fit when modelling one migration event
159 (admixture weight = 42%; residuals <2x SE) (Supplementary section 8), indicating that part of
160 the Columbian mammoth's ancestry is derived from the Krestovka lineage.

161 To further assess the evolutionary context of the Krestovka lineage within the population history
162 of mammoths, we used two complementary admixture graph model approaches^{22,23}. We
163 exhaustively tested all possible phylogenetic combinations relating the three ancient individuals
164 with one Siberian woolly mammoth, one Columbian mammoth and one Asian elephant. We set
165 the latter as outgroup, only including sites identified as polymorphic in six Asian elephant
166 genomes to limit the effects of incorrectly called genotypes (Supplementary Section 8). None of
167 the graph models without admixture events provided good fits to the data, thus ruling out a
168 simple tree-like population history. In contrast, graph models with just one admixture event
169 provided a perfect fit, explaining all 45 f_4 -statistic combinations without significant outliers.
170 Based on the point estimates obtained from the two different admixture graph model
171 approaches, the Columbian mammoth is estimated to be the result of an admixture event where
172 38-43% of its ancestry was derived from a lineage related to Krestovka, and 57-62% from the
173 woolly mammoth lineage (Fig. 2b, Extended Data Fig. 6).

174 We obtained additional support for the complex ancestry of the Columbian mammoth by
175 employing a hidden Markov model aimed at identifying admixed genomic regions from an
176 unknown source (*i.e.* ghost admixture)²⁴ (Supplementary Section 9). This analysis, which was
177 done without including any of the Early and Middle Pleistocene specimens, suggested that
178 roughly 41% of the Columbian mammoth genome originates from a lineage genetically
179 differentiated from the woolly mammoth (Extended Data Fig. 7a). We subsequently built
180 pairwise-distance phylogenetic trees for the genomic regions identified as being the result of
181 ghost admixture and found them closely related to the Krestovka genome (Extended Data Fig.
182 7b, Supplementary Section 9). In contrast, when excluding these regions, the remaining part of
183 the Columbian mammoth genome falls within the diversity of Late Pleistocene woolly
184 mammoths (Extended Data Fig. 7c, Supplementary Section 9).

185 Finally, our D-statistics analysis also identified higher levels of derived allele sharing between
186 the Columbian mammoth and a woolly mammoth from Wyoming (Fig. 2a). Based on f_4 -ratios,
187 we estimate 10.7-12.7% excess shared ancestry between these genomes (Supplementary
188 Section 9), consistent with an earlier study¹⁵. Since the Columbian mammoth carries a large
189 proportion of Krestovka ancestry, gene flow from the Columbian mammoth into North American
190 woolly mammoths would have resulted in a larger proportion of allele sharing between
191 Krestovka and the Wyoming woolly mammoth. Our finding of no excess allele sharing between
192 the Krestovka genome and any of the sequenced woolly mammoths, including the individual
193 from Wyoming (Supplementary Table 7), therefore indicates that this second phase of gene flow
194 may have been unidirectional, from woolly mammoth into the Columbian mammoth. This implies
195 that the composition of the Columbian mammoth's genome, as identified in the D-statistics,
196 admixture graph models, and ghost-admixture analysis, is the result of two admixture events,
197 where an initial ~50% contribution from each of the Krestovka and woolly mammoth lineages
198 was followed by an additional ~12% gene flow from North American woolly mammoths (Fig. 2c).

199 **Insights into mammoth adaptive evolution**

200 The woolly mammoth evolved into a cold-tolerant, open-habitat specialist through a series of
201 adaptive changes⁸. The antiquity of our genomes makes it possible to investigate when these
202 adaptations evolved. To do this, we identified protein-coding changes for which all Late
203 Pleistocene woolly mammoths carried the derived allele and all African and Asian elephants
204 carried the ancestral allele (n = 5,598; Supplementary Table 8). Among the variants that could
205 be called in the Early and Middle Pleistocene genomes, we find that 85.2% (782 out of 918) and
206 88.7% (2,578 out of 2,906) of the mammoth-specific protein-coding changes were already
207 present in the genomes of Adycha (*trogontherii*-like) and Chukochya (early woolly mammoth),
208 respectively (Supplementary Section 10, Supplementary Table 9). Moreover, we did not detect
209 significant differences in the ratio of shared non-synonymous versus synonymous sites among
210 our sequenced Early, Middle, and Late Pleistocene genomes (Supplementary Table 9). Thus,
211 despite the transitions in climate and mammoth morphology at the onset of the Middle
212 Pleistocene, we do not observe any marked change in the rate of protein-coding mutations
213 during this time period.

214 Previous analyses have identified specific genetic changes that are thought to underlie a suite
215 of woolly mammoth adaptations to the Arctic environment²⁵. For these variants (n = 91), we
216 assessed whether the Adycha and Chukochya genomes shared the same amino acid changes
217 as those observed in Late Pleistocene woolly mammoths (Supplementary Table 10). We find
218 that among genes possibly involved in hair growth, circadian rhythm, thermal sensation, and
219 white and brown fat deposits, the vast majority of coding changes were present in both the
220 Adycha (87%) and Chukochya (89%) genomes (Supplementary Table 10). This suggests that
221 Siberian *trogontherii*-like mammoths (i.e. Adycha) had already developed a woolly fur as well as
222 several physiological adaptations to a cold high-latitude environment (Supplementary Section
223 11). However, in one of the best studied genes in the woolly mammoth, *TRPV3*, which encodes
224 a temperature-sensitive transient receptor channel, potentially involved in thermal sensation and
225 hair growth²⁵, we find that only two out of four amino-acid changes identified in Late Pleistocene
226 woolly mammoths were present in the early woolly mammoth genome (Chukochya). This
227 indicates that non-synonymous changes in this gene occurred over several hundreds of
228 thousands of years, rather than during a single brief burst of adaptive evolution.

229 **Discussion**

230 Our genomic analyses suggest that the Columbian mammoth is a product of admixture between
231 woolly mammoths and a previously unrecognised ancient mammoth lineage represented by the
232 Krestovka specimen. Given the finding that each of these lineages initially contributed roughly
233 half of their genome to this ancient admixture, we propose that the origin of the Columbian
234 mammoth constitutes a hybrid speciation event²⁶. This hybridisation event appears not to have
235 imparted any shift in average molar morphology of North American populations¹⁰, but can
236 explain the mitochondrial-nuclear discordance in the Columbian mammoth¹⁸ where all known
237 Columbian mammoth mitogenomes are nested within the woolly mammoth's mitogenome
238 diversity (Fig. 1c). Based on the mitogenome phylogeny, we estimate that the most recent
239 common female ancestor of all Late Pleistocene Columbian mammoths lived approximately 420
240 ka (95% HPD 511 - 338 ka), providing a likely minimum age for when this hybridization event

241 occurred (Fig. 1c). Since mammoths had already appeared in North America by 1.5 Ma, these
242 findings imply that prior to the hybridisation event, North American mammoths belonged to the
243 Krestovka lineage. Given the morphology of the Krestovka specimen, this corroborates the
244 model proposed by Lister & Sher¹⁰ that the earliest North American mammoths were derived
245 from a *trogontherii*-like Eurasian ancestor, rather than originating from an expansion of the
246 southern mammoth (*M. meridionalis*) into North America²⁷.

247 Our findings demonstrate that genomic data can be recovered from Early Pleistocene
248 specimens, opening up the possibility of studying adaptive evolution across speciation events.
249 The mammoth genomes presented here offer a glimpse of this potential. Even though the
250 transition from *trogontherii*-like (Adycha) to woolly (Chukochya) mammoths represents a
251 significant change in molar morphology (Extended data Fig. 1), we do not observe an increased
252 rate of genome-wide selection during this time period. Moreover, many key adaptations
253 identified in Late Pleistocene mammoth genomes were already present in the Early Pleistocene
254 Adycha genome. We thus find no evidence for an increased rate of adaptive evolution
255 associated with the origin of the woolly mammoth. This is consistent with previous work
256 suggesting that the major shift in habitat and morphology of mammoths happened earlier,
257 between *meridionalis*-like and *trogontherii*-like mammoths^{8,10}.

258 The retrieval of DNA older than one million years confirms previous theoretical predictions¹ that
259 the ancient genetic record can be extended beyond what has been previously shown. We
260 anticipate that additional recovery and analyses of Early and Middle Pleistocene genomes will
261 further improve our understanding of the complex nature of evolutionary change and speciation.
262 Our results highlight the importance of perennially frozen environments for extending the
263 temporal limits of DNA recovery, and hint at a future deep-time chapter of ancient DNA research
264 that will likely be predominantly fueled by specimens from high latitudes.

265 **References (Main)**

- 266 1. Allentoft, M. E. *et al.* The half-life of DNA in bone: measuring decay kinetics in 158
267 dated fossils. *Proc. Biol. Sci.* **279**, 4724–4733 (2012).
- 268 2. Orlando, L. *et al.* Recalibrating Equus evolution using the genome sequence of an early
269 Middle Pleistocene horse. *Nature* **499**, 74–78 (2013).
- 270 3. Skoglund, P. *et al.* Origins and genetic legacy of Neolithic farmers and hunter-gatherers
271 in Europe. *Science* **336**, 466–469 (2012).
- 272 4. Green, R. E. *et al.* A draft sequence of the Neandertal genome. *Science* **328**, 710–722
273 (2010).
- 274 5. Palkopoulou, E. *et al.* Complete genomes reveal signatures of demographic and genetic
275 declines in the woolly mammoth. *Curr. Biol.* **25**, 1395–1400 (2015).
- 276 6. Weir, J. T. & Schlüter, D. Ice sheets promote speciation in boreal birds. *Proc. Biol. Sci.*
277 **271**, 1881–1887 (2004).
- 278 7. Lister, A. M. The impact of Quaternary Ice Ages on mammalian evolution. *Philos. Trans. R. Soc. Lond. B Biol. Sci.* **359**, 221–241 (2004).
- 280 8. Lister, A. M., Sher, A. V., van Essen, H. & Wei, G. The pattern and process of mammoth
281 evolution in Eurasia. *Quaternary International* vols 126-128 49–64 (2005).
- 282 9. *Cenozoic Mammals of Africa*. (University of California Press, 2010).
- 283 10. Lister, A. M. & Sher, A. V. Evolution and dispersal of mammoths across the Northern
284 Hemisphere. *Science* **350**, 805–809 (2015).
- 285 11. Repenning, C. A. *Allophaiomys and the Age of the Olyor Suite, Krestovka Sections, Yakutia*. (U.S. Government Printing Office, 1992).
- 287 12. Dabney, J. *et al.* Complete mitochondrial genome sequence of a Middle Pleistocene
288 cave bear reconstructed from ultrashort DNA fragments. *Proc. Natl. Acad. Sci. U. S. A.*
289 **110**, 15758–15763 (2013).
- 290 13. Briggs, A. W. *et al.* Removal of deaminated cytosines and detection of in vivo
291 methylation in ancient DNA. *Nucleic Acids Res.* **38**, e87 (2010).
- 292 14. Meyer, M. & Kircher, M. Illumina sequencing library preparation for highly multiplexed
293 target capture and sequencing. *Cold Spring Harb. Protoc.* **2010**, db.prot5448 (2010).

294 15. Palkopoulou, E. *et al.* A comprehensive genomic history of extinct and living elephants.
295 *Proc. Natl. Acad. Sci. U. S. A.* **115**, E2566–E2574 (2018).

296 16. Rohland, N. *et al.* Proboscidean mitogenomics: chronology and mode of elephant
297 evolution using mastodon as outgroup. *PLoS Biol.* **5**, (2007).

298 17. Meyer, M. *et al.* A high-coverage genome sequence from an archaic Denisovan
299 individual. *Science* **338**, 222–226 (2012).

300 18. Chang, D. *et al.* The evolutionary and phylogeographic history of woolly mammoths: a
301 comprehensive mitogenomic analysis. *Sci. Rep.* **7**, 44585 (2017).

302 19. Pečnerová, P. *et al.* Mitogenome evolution in the last surviving woolly mammoth
303 population reveals neutral and functional consequences of small population size. *Evol/*
304 *Lett* **1**, 292–303 (2017).

305 20. Barnes, I. *et al.* Genetic structure and extinction of the woolly mammoth, *Mammuthus*
306 *primigenius*. *Curr. Biol.* **17**, 1072–1075 (2007).

307 21. Pickrell, J. K. & Pritchard, J. K. Inference of population splits and mixtures from genome-
308 wide allele frequency data. *PLoS Genet.* **8**, e1002967 (2012).

309 22. Patterson, N. *et al.* Ancient admixture in human history. *Genetics* **192**, 1065–1093 (2012).

310 23. Leppälä, K., Nielsen, S. V. & Mailund, T. admixturegraph: an R package for admixture
311 graph manipulation and fitting. *Bioinformatics* **33**, 1738–1740 (2017).

312 24. Skov, L. *et al.* Detecting archaic introgression using an unadmixed outgroup. *PLoS*
313 *Genet.* **14**, e1007641 (2018).

314 25. Lynch, V. J. *et al.* Elephantid Genomes Reveal the Molecular Bases of Woolly Mammoth
315 Adaptations to the Arctic. *Cell Rep.* **12**, 217–228 (2015).

316 26. Mallet, J. Hybrid speciation. *Nature* **446**, 279–283 (2007).

317 27. Lucas, S. G., Morgan, G. S., Love, D. W. & Connell, S. D. The first North American
318 mammoths: Taxonomy and chronology of early Irvingtonian (Early Pleistocene)
319 *Mammuthus* from New Mexico. *Quat. Int.* **443**, 2–13 (2017).

320 **Figure legends**

321

322 **Fig. 1. DNA-based phylogenies and specimen age estimates.** **a**, Geographic origin of the
323 mammoth genomes analysed in this study. **b**, Phylogenetic tree built in FASTME based on
324 pairwise genetic distances, assuming balanced minimum evolution using all nuclear sites as
325 well as 100 resampling replicates based on 100,000 sites each. **c**, Bayesian reconstruction of
326 the mitochondrial tree, with the molecular clock calibrated using radiocarbon dates of ancient
327 samples for which a finite radiocarbon date was available, as well as assuming a lognormal
328 prior on the divergence between the African savannah elephant (not shown in the tree) and
329 mammoths with a mean of 5.3 Ma. Blue bars reflect 95% highest posterior densities. Circles
330 depict the position of the newly sequenced genomes. **d**, Densities for age estimates of samples
331 Adycha and Chukochya based on autosomal divergence to African savannah elephant (*L.*
332 *africana*) and **e**, Densities for age estimates of samples Krestovka, Adycha and Chukochya
333 based on mitochondrial genomes as inferred from the Bayesian mitochondrial reconstruction.

334

335 **Fig. 2. Inferred genomic history of mammoths.** **a**, D-statistics where each dot reflects a
336 comparison involving one woolly mammoth genome and one genome depicted on the right side
337 of the panel (where *L. africana* = African savannah elephant, *P. antiquus* = straight-tusked
338 elephant, *Mammuthus sp.* = all mammoth specimens in this study, *M. columbi* = Columbian
339 mammoth, and *M. primigenius* = woolly mammoth), iterating through all possible sample
340 combinations using the mastodon (*Mammut americanum*) as an outgroup. No elevated allele
341 sharing between any of the mammoth genomes and the reference (African savannah elephant)
342 is observed, suggesting no pronounced reference biases in the Early/Middle Pleistocene
343 genomes. A strong affinity between Columbian mammoths and sample Krestovka is observed,
344 as well as a relationship between the North American woolly mammoth (Wyoming) and the
345 Columbian mammoth. **b**, Best fitting admixture graph model for one admixture event,
346 suggesting a hybrid origin for the Columbian mammoth. **c**, Hypothesized evolutionary history of
347 mammoths during the last 3 Ma, based on currently available genomic data. Brown dots
348 represent mammoth specimens for which genomic data has been analysed in this study, with
349 error bars representing 95% highest posterior density intervals from the mitogenome-based age
350 estimates obtained for the three Early and Middle Pleistocene specimens. Arrows depict gene
351 flow events identified from the autosomal genomic data. The European steppe mammoth (*M.*
352 *trogontherii*) survived well into the later stages of the Middle Pleistocene, and we hypothesize
353 that it most likely branched off from a common ancestor shared with the woolly mammoth at ~1
354 Ma.

355

356

357 **Methods**

358 **Morphometry of mammoth molars**

359 Mammoth molars were measured according to the method described in Lister & Sher¹⁰
360 (Supplementary Section 1). Samples considered are as follows: *Mammuthus meridionalis*, ca.
361 2.0 Ma, Upper Valdarno, Italy (type locality) (n=34); *M. trogontherii*, ca. 0.6 Ma, Süssenborn,
362 Germany (type locality) (n=48); *M. primigenius*, Late Pleistocene of North-East Siberia (Russia)
363 and Alaska (USA) (n=28). Early (n=8) and Late (n=15) Olyorian samples are from localities in
364 the Yana-Kolyma lowland (Early Olyorian is ~1.2 – 0.8 Ma, Late Olyorian is 0.8 – 0.5 Ma;
365 Extended Data Fig. 2). North American Early to early Middle Pleistocene samples (ca. 1.5 – 0.5
366 Ma) are from Old Crow (Yukon, Canada), Leisey Shell Pit 1A and Punta Gorda (Florida, USA),
367 and the Ocotillo Formation (California, USA) (combined n=16). Original data are from Lister &
368 Sher¹⁰, where further details on sites and collections can be found.

369 **DNA extraction and sequencing**

370 Samples from Early-Middle Pleistocene mammoth molars (Krestovka, Adycha, Chukochya) as
371 well as Late Pleistocene samples (Scotland, Kanchalan) were processed in dedicated ancient
372 DNA laboratories following standard ancient DNA practices (Supplementary Section 2).
373 Following DNA extraction¹², we constructed double- or single-stranded Illumina libraries^{14,28},
374 which were treated to remove uracils caused by post-mortem cytosine deamination¹³. We
375 subsequently sequenced these libraries using Illumina platforms, generating from 200 to 2,350
376 million paired-end reads (2x 50 or 2x150 bp) per specimen (Supplementary Table 1).

377 **Sequence data processing and mapping**

378 We combined our sequence data with previously published genomic data from elephantids
379 generated by Palkopoulou *et al.*¹⁵ (Supplementary Table 2). For the five samples sequenced in
380 this study, we trimmed adapters and merged paired-end reads using SeqPrep v1.1²⁹, initially
381 retaining reads either ≥ 25 bp (Krestovka, Adycha, Chukochya) or ≥ 30 bp (Scotland, Kanchalan),
382 and with a minor modification in the source code that allowed us to choose the best base quality
383 score in the merged region instead of aggregating the scores⁵ (Supplementary Section 3). For
384 genomic data from the straight-tusked elephant, and the Scotland and Kanchalan mammoths,
385 which had been treated with the afu UDG enzyme leaving post-mortem DNA damage at the
386 ends of the molecules (Supplementary Tables 2 and 3), we removed the first and last two base
387 pairs from all reads before mapping. The merged reads were mapped to a composite reference,
388 consisting of the African savannah elephant nuclear genome (LoxAfr4), woolly mammoth
389 mitogenome (DQ188829), and the human genome (hg19) using BWA aln v0.7.8 with
390 deactivated seeding (-l 16,500), allowing for more substitutions (-n 0.01) and up to two gaps (-o
391 2)^{30,31}. The human genome was included as a decoy to filter out spurious mappings in genomic
392 conserved regions³². Next, we removed PCR duplicates from the alignments using a custom
393 python script⁵. After obtaining initial quality metrics for the genomes, we removed reads < 35
394 base pairs from the BAM-files using samtools v1.10³³ and awk for all remaining analysis
395 (Supplementary Section 4).

396 **Ancient DNA authenticity and quality assessment**

397 All ancient genomes were treated to reduce post-mortem DNA damage. For the most ancient
398 samples (Krestovka, Adycha, Chukochya), we took several steps to assess the authenticity and
399 quality of the data (Supplementary Section 4). First, only reads that mapped uniquely to non-
400 repetitive regions of the LoxAfr4 reference and had a mapping quality ≥ 30 were retained,
401 whereas reads that mapped equally well to the human genome reference (hg19) in our
402 composite reference were removed to reduce possible biases caused by contaminant human
403 reads³². Second, we employed a method based on the rate of mismatches per base pair to the
404 reference to assess the rate of spurious mappings for all reads between 20-35 bp and at 5 bp
405 intervals between 35-50 bp (Supplementary Section 4). This allowed us to identify a sample-
406 specific minimum read length cutoff, above which we consider reads to be correctly mapped
407 and endogenous (Supplementary Section 4, Supplementary Table 3). Based on this, we applied
408 the longest sample-specific cutoff (≥ 35 bp, Krestovka) for all samples. We used mapDamage
409 v2.0.6³⁴ to obtain read length distributions for all ancient samples. Finally, an assessment of
410 cytosine deamination profiles at CpG sites, which are unaffected by UDG treatment¹³, was done
411 using the *platypus* option in PMDtools (github.com/pontussk/PMDtools)³⁵. A full set of ancient
412 DNA quality statistics are available in Supplementary Tables 1-3.

413 **Allele sampling**

414 To minimize coverage-related biases, all subsequent analyses were based on pseudo-
415 haploidized sequences that were generated by randomly selecting a single high quality base
416 call at each autosomal genomic site using ANGSD v0.921³⁶. For base calling we only
417 considered reads ≥ 35 bp, a mapping and base quality ≥ 30 , and reads without multiple best hits
418 (-uniqueOnly 1). Finally, we masked all sites within repetitive regions as identified with
419 RepeatMasker v.4.0.7³⁷, CpG sites, sites with more than two alleles among all individuals, and
420 sites with coverage above the 95th percentile of the genome-wide average to reduce false calls
421 from duplicated genomic regions.

422 **Reconstruction of mitogenomes, tip-dating, and mtDNA phylogeny**

423 Mitochondrial genomes for the five newly sequenced samples were assembled using MIA³⁸ with
424 the Asian elephant (NC_005129)¹⁶ mitogenome as reference for Adycha, Krestovka, and
425 Chukochya and the mammoth mitogenome (NC_007596) as reference for the Late Pleistocene
426 woolly mammoth samples from Scotland and Kanchalan, restricting the input reads to those ≥ 35
427 bp for each (Supplementary Section 5). This yielded mitochondrial assemblies with coverage of
428 37.8x, 47.5x, and 77.1x for Adycha, Krestovka, and Chukochya, and 99.6x and 179.5x for
429 Scotland and Kanchalan, respectively. These assemblies were then aligned using Muscle
430 v3.8.31³⁹ together with previously published elephantid mitogenomes^{18,19,40}. Following alignment
431 partitioning, the HKY model with a gamma-distributed rate heterogeneity⁴¹ and a proportion of
432 invariant sites or just a proportion of invariant sites, was identified as best-fitting for each
433 alignment partition using jModelTest v2.1.10⁴² (Supplementary Section 5). To estimate the age
434 of the three oldest *Mammuthus* samples (Adycha, Krestovka, Chukochya), we performed a
435 Bayesian reconstruction of the phylogenetic tree using BEAST v1.10.4⁴³. We calibrated the
436 molecular clock using tip ages for all ancient samples with a finite radiocarbon date, as well as a
437 lognormal prior of 5.3 Ma on the genetic divergence of *Loxodonta* and *Elephas/Mammuthus* as
438 obtained from previous genomic studies¹⁵ (Supplementary Table 4). In addition, we tested for an

439 older divergence (7.6 Ma) between *Loxodonta* and *Mammuthus* that is more consistent with the
440 fossil record¹⁶ (see Supplementary Section 5). For both priors, we used a standard deviation of
441 500,000 years. We assumed a strict molecular clock and the flexible skygrid coalescent model⁴⁴
442 to account for the complex cross-generic demographic history of the included taxa. The ages of
443 all samples beyond the limit of radiocarbon dating were estimated by sampling from lognormal
444 distributions with priors based on stratigraphic context and previous genetic studies, using two
445 MCMC chains of 100 million generations, sampling every 10,000 and discarding the first 10% as
446 burn-in (Supplementary Table 5, Supplementary Section 5).

447 **Genetic dating based on autosomal data**

448 Specimen age estimates for Adycha and Chukochya (Krestovka was excluded as too few
449 autosomal bases were available for this analysis) were estimated based on the autosomal data
450 following the method described in Meyer *et al.*¹⁷, using the American mastodon (*Mammut*
451 *americanum*), which is an outgroup to all elephantids, and the African savannah and Asian
452 elephant genomes as outgroups. We inferred the ancestral state for a given base in the African
453 elephant reference genome by requiring that the alignments of the mastodon, two African
454 elephants and five Asian elephants are present and identical at that nucleotide. We used the
455 high coverage and radiocarbon dated Wrangel Island woolly mammoth genome as a calibration
456 point⁵. Each difference to the ancestral state was then counted for the Wrangel genome and the
457 focal *Mammuthus* genome for all sites at which both genomes had a called base. We calculated
458 the relative age of each individual as $(nW - nM)/nW$, based on the number of derived changes
459 in the Wrangel genome (nW) and the other *Mammuthus* genome (nM), using an assumed
460 divergence time of 5.3 million years¹⁵ to the common ancestor of African elephant and woolly
461 mammoth. Age variance estimates were calculated in windows of 5 Mb and we computed
462 bootstrap confidence intervals as 1.96× standard error around the date estimates
463 (Supplementary Section 6).

464 **Nuclear genetic relationships and phylogeny**

465 We reconstructed phylogenetic trees based on the whole genome Identical-By-State (IBS)
466 matrix for all individuals using the “doIBS” function in ANGSD. We calculated pairwise genetic
467 distances between individuals using the full dataset, as well as 100 resampling replicates based
468 on 100,000 sites each. Second, we obtained the phylogenetic tree using a balanced minimum
469 evolution (ME) method as implemented in FASTME⁴⁵ (Fig. 1b, Supplementary Section 7). Next,
470 we inferred relative population split times using an approach that examines single nucleotide
471 polymorphic (SNP) positions that are heterozygous in an individual from one population and
472 measures the fraction of these sites at which a randomly sampled allele from an individual of a
473 second population carries the derived variant, polarized by an outgroup ($F(A|B)$ statistics)⁴. We
474 ascertained heterozygous sites in three high-coverage genomes — *E. maximus* and *M.*
475 *primigenius* (Oimyakon and Wrangel)⁵ — using the SAMtools v.1.10³³ ‘mpileup’ command and
476 bcftools. We only included SNPs with a quality ≥ 30 , and filtered out all SNP in repetitive regions,
477 within 5 bp from indels, at CpG sites and sites below 1/3 or above two times the genome-wide
478 average coverage. For each of the *Mammuthus* genomes, we then estimated the proportion of
479 sites for which a randomly drawn allele at the ascertained heterozygous sites matches the
480 derived state.

481 **D, f4 statistics, AdmixtureGraphs and TreeMix**

482 We first used Admixtools v5²² to calculate D- and f_4 -statistics for all possible quadruple
483 combinations of samples iterating through the three different groups (P_1 , P_2 , P_3) based on the
484 randomly sampled alleles, conditioning on all sites that are polymorphic among the 6 Asian
485 elephant genomes²². The mastodon was used as an outgroup in all comparisons
486 (Supplementary Table 6, 7). Direct estimates of genomic ancestries using f_4 -ratios were
487 additionally calculated for specific pairs in AdmixTools (Supplementary section 9)²². Second, we
488 used the admixturegraph R package²³ to assess the genetic relationship among the
489 *Mammuthus* genomes using admixture graph models, fitting graphs to all possible f_4 -statistics
490 involving a given set of genomes. To resolve the relationships of the Adycha, Krestovka and
491 Chukochya individuals within the population history of mammoths, we exhaustively tested all
492 135,285 possible admixture graphs (with up to two admixture events) relating these three
493 individuals, one woolly mammoth (Wrangel), one Columbian mammoth, and one Asian
494 elephant, setting the latter as outgroup (Supplementary Section 8). We repeated the
495 admixturegraph analysis using the above described f_4 -statistic with qpBrute⁴⁶, which in addition
496 allowed us to estimate shared genetic drift and branch lengths using f_2 and f_3 statistics. At each
497 step, insertion of a new node was tested at all branches of the graph, except the outgroup
498 branch. Where a node could not be inserted without producing f_4 outliers (i.e. $|Z| >= 3$), all
499 possible admixture combinations were also attempted. The resulting list of all fitted graphs was
500 then passed to the MCMC algorithm implemented in the admixturegraph R package, to compute
501 the marginal likelihood of the models and their Bayes Factors. Finally, we estimated genetic
502 relationships and admixture among the *Mammuthus* samples using TreeMix v1.12²¹. We first
503 estimated the allele frequencies among the randomly sampled alleles and subsequently ran the
504 TreeMix model accounting for linkage disequilibrium (LD) by grouping sites in blocks of 1,000
505 SNPs (-k 1,000) setting the *E. maximus* samples as root. Standard errors (-SE) and bootstrap
506 replicates (-bootstrap) were used to evaluate the confidence in the inferred tree topology. After
507 constructing a maximum-likelihood tree, migration events were added (-m) and iterated 10
508 times for each value of m (1–10) to check for convergence in the likelihood of the model as well
509 as the explained variance following each addition of a migration event. The inferred maximum-
510 likelihood trees were visualized with the in-built TreeMix R script plotting functions.

511 **Introgression in the Columbian mammoth**

512 We further tested for admixture in the Columbian and Scotland mammoths using a hidden
513 Markov model²⁴. This method identifies genomic regions within a given individual that possibly
514 came from an admixture event with a distant lineage not present in the dataset based on the
515 distribution of private sites. Briefly, we estimated the number of callable sites, the SNP density
516 (as a proxy for per-window mutation rate) and the number of private variants with respect to all
517 other elephant genomes except Krestovka in 1 kb windows. We applied settings without gene
518 flow, or with one gene flow event with starting probabilities and decoding described in
519 Supplementary Section 9. We tested for ghost admixture in the Columbian mammoth using
520 sites private to the Columbian mammoth with respect to all other genomes in this study except
521 Krestovka. We subsequently obtained fasta-alignments for those autosomal regions identified
522 as “unadmixed” and “ghost-admixed” in the Columbian mammoths by calling a random base at

523 each covered position using ANGSD. Minimal evolution phylogenies were then obtained for
524 both alignments as described in the 'Nuclear genetic relationships and phylogeny' section.

525 **Genetic adaptations of the woolly mammoth**

526 To investigate the timing of genetic adaptations in the woolly mammoth lineage, we used *last*
527 v1170⁴⁷ to build a chain file to lift over our sampled allele dataset mapped to LoxAfr4 to the
528 annotated LoxAfr3 reference genome. Following construction of a reference index using *lastdb*
529 (-P0 -uNEAR -R01), we aligned the two references using *lastal* (-m50 -E0.05 -C2). The
530 alignment was converted to MAF format (*last-split -m1*) and finally to a chain file with the *maf-*
531 *convert* tool (last.cbrc.jp). The Picard Liftover tool ('Picard Toolkit', 2019) was then used to lift
532 over the identified variants to the LoxAfr3 reference. Using the African savannah elephant
533 genome annotation (LoxAfr3.gff), we identified all amino-acid changes where all Late
534 Pleistocene woolly mammoth genomes carry the derived state and all other elephantid
535 genomes carry the ancestral allele using VariantEffectPredictor⁴⁸. For all identified amino-acid
536 changes, we assessed the state (derived or ancestral) among the three oldest samples
537 (Krestovka, Adycha, Chukochya) and the Columbian mammoth (Supplementary Table 8-10). In
538 addition, we conducted a Gene Ontology enrichment on all genes for which the woolly
539 mammoth genomes (including Chukochya and Adycha) are derived, using GOrilla⁴⁹. Finally, we
540 used PAML v1.3.1⁵⁰ to identify genes that potentially have been under positive selection in Late
541 Pleistocene woolly mammoths (Supplementary Table 11, Supplementary Section 10).

542 **Extended Data figure legends**

543

544 **Extended Data Fig. 1. Mammoth molars and morphometric comparisons.** **a-b**, upper third
545 molars in lateral and cross-sectional views; **c**, partial lower third molar in lateral and occlusal
546 views. **a**, Chukochya (PIN-3341-737); **b**, Krestovka (PIN-3491-3) flipped horizontally; **c**,
547 Adycha (PIN-3723-511), occlusal view flipped horizontally. Note the more closely-spaced
548 lamellae and thinner enamel in **a** (*primigenius*-like) than **b** and **c** (*trogontherii*-like). **d**,
549 Hypsodonty index vs lamellar length index of upper M3s; **e**, Enamel thickness index vs basal
550 lamellar length index of lower M3s. Olyorian specimens yielding DNA are labelled by site name.
551 Green dashed line: convex hull summarising Early to early Middle Pleistocene (ca. 1.5-0.5 Ma)
552 North American *Mammuthus* samples (data points not shown). Green and blue squares: Early
553 and Late Olyorian North-East Siberian samples, respectively; red and green circles: European
554 *M. meridionalis* and *M. trogontherii*, respectively; blue circles, *M. primigenius* from North-East
555 Siberia and Alaska. Note (i) similarity of Krestovka and Adycha to other Early Olyorian molars
556 and to European steppe mammoths (*M. trogontherii*), (ii) similarity of early North American
557 mammoths to these (Early Olyorian in particular), (iii) similarity of Chukochya to *M. primigenius*.
558 For site details, measurement definitions and data, see Supplementary Section 1.

559

560 **Extended Data Fig. 2. Sample age based on biostratigraphy, paleomagnetic reversals and**
561 **genomic data.** Chart shows the stratigraphic position of the Kutuyakhian fauna, *Phenacomys*
562 complex, Early Olyorian and Late Olyorian faunas in relation to important European, northwest
563 Asian and northern North American stratigraphic benchmarks. ELMA - European Land Mammal
564 Ages (small mammals), LMA - Land Mammal Ages (large mammals), MN/MQ - European
565 Small Mammal Biozones, EEBU – East European biochronological units. Biostratigraphic and
566 palaeomagnetic based chronological constraints for the specimens are provided, in comparison
567 with the DNA-based age estimations.

568

569 **Extended Data Fig. 3. DNA fragment length distributions for nine mammoths.** Reads are
570 aligned to the LoxAfr4 autosomes. For the three Early-Middle Pleistocene samples (Krestovka,
571 Adycha, Chukochya), reads of 25-200 bp length are shown, whereas 30-200 bp reads are
572 shown for the remaining samples. Ultrashort reads (<35 bp) are denoted in red and were shown
573 to be enriched for spurious alignments and therefore excluded from downstream analyses
574 (Supplementary Section 4). The mean read lengths (μ) were calculated using only the retained
575 reads (≥ 35 bp).

576

577 **Extended Data Fig. 4. Post-mortem cytosine deamination damage profiles at CpG sites.**
578 The most ancient samples (Krestovka, Adycha, Chukochya) carry a greater frequency of
579 cytosine deamination compared to younger permafrost preserved woolly mammoth samples
580 (Oimyakon and Wrangel) and the Columbian mammoth (*M. columbi*) specimen.

581

582 **Extended Data Fig. 5. F(A|B) statistics.** The statistics reflect relative divergence between the
583 genomes on the left and the right side. Lower values indicate reduced derived allele sharing
584 between the sample indicated on the left and the right of the graph, at sites for which the

585 genome on the right panel is heterozygous. The lower the value, the more drift has occurred
586 between the genomes and thus the older their genetic divergence.

587

588 **Extended Data Fig. 6. qpGraph model.** The most parsimonious graph model (highest Bayes
589 Factor) of the phylogenetic relationships among mammoths lineages augmented with one
590 admixture event. Branch lengths are given in f-statistic units multiplied by 1,000. Discontinuous
591 lines show admixture events between lineages, with percentages representing admixture
592 proportions.

593

594 **Extended Data Fig. 7. Ghost introgression analysis of the Columbian mammoth genome.**

595 **a**, The number of private alleles per 1000 bp within genomic regions identified as woolly
596 mammoth (*M. primigenius*) ancestry or ghost ancestry. **b**, Maximum-likelihood phylogenies for
597 those genomic regions identified as ghost ancestry in the Colombian mammoth (*M. columbi*)
598 genome. **c**, Maximum-likelihood phylogenies for regions identified as un-admixed ancestry.

599

600 Acknowledgments

601 T.v.d.V, P.P. and D.D.d.M., M.D. and L.D. acknowledge support from the Swedish Research
602 Council (2012-3869 & 2017-04647), FORMAS (2018-01640) and the Tryggers Foundation (CTS
603 17:109). A.G. is supported by the Knut and Alice Wallenberg Foundation (1,000 Ancient
604 Genomes project). A.B. and P.S. were supported by the Francis Crick Institute (FC001595)
605 which receives its core funding from Cancer Research UK, the UK Medical Research Council,
606 and the Wellcome Trust. P.S. was supported by the European Research Council (grant no.
607 852558), the Wellcome Trust (217223/Z/19/Z), and the Vallee Foundation. MH, JAT and GX
608 were supported by NERC (grant no. NE/J009490/1) and the ERC StG grant GeneFlow
609 (#310763). B.S. and J.O. were supported by the U.S. National Science Foundation (DEB-
610 1754451). P.N. was supported by RFBR (grant no. 13-05-01128). The authors also
611 acknowledge support from Science for Life Laboratory, the Knut and Alice Wallenberg
612 Foundation, the National Genomics Infrastructure funded by the Swedish Research Council,
613 and Uppsala Multidisciplinary Center for Advanced Computational Science for assistance with
614 massively parallel sequencing and access to the UPPMAX computational infrastructure. Neil
615 Clark at the Hunterian Museum kindly provided access to the Scotland mammoth sample.
616 Finally, we wish to especially acknowledge the seminal work of our late friend and colleague
617 Andrei Sher, who in many years of fieldwork defined and described the Olyorian sequence,
618 collected large quantities of fossil vertebrate material including all the Early/Middle Pleistocene
619 specimens studied here, and consistently promoted multidisciplinary studies on his finds.

620 Author contributions

621 L.D., A.M.L., B.S., M.H and I.B. conceived the project. L.D., A.G., P.P. and D.D.d.M. designed
622 the study together with P.N. and A.M.L.. Laboratory work on Early/Middle Pleistocene samples
623 was done by P.P., L.D., A.G. and M.D., and G.X. and J.A.T. conducted laboratory work on Late
624 Pleistocene samples. P.P., T.v.d.V. and D.D.d.M. processed and mapped sequence data.
625 T.v.d.V., S.H. and P.D.H. performed tests on DNA authenticity. T.v.d.V., J.O. and S.L.

626 conducted phylogenetic and Treemix analyses. J.O. and T.v.d.V. computed genomic age
627 estimates. T.v.d.V., A.B. and D.D.d.M. performed analyses on D- and f4-statistics and admixture
628 graph models. T.v.d.V. performed analyses on population structure, and ghost admixture.
629 T.v.d.V., E.S., F.R.F. and M.S. performed analysis on selection. L.D., P.D.H., M.H., B.S., A.G.,
630 M.S., P.S. P.N. and A.M.L. provided advice on the bioinformatic analyses and/or helped
631 interpret the results. Morphological analyses as well as palaeontological and geological
632 information was provided by P.N. and A.M.L. The manuscript was written by T.v.d.V., P.P.,
633 D.D.d.M., P.N. and L.D., with contributions from all coauthors.

634 **Data Availability**

635

636 All sequence data (in fastq format) for samples sequenced in this study are available through
637 the European Nucleotide Archive under accession number PRJEB42269. Previously published
638 data used in this study are available under accession numbers PRJEB24361 and PRJEB7929.

639 **Code availability**

640 The custom code used in this study to evaluate read length cut-offs is available from
641 github.com/stefaniehartmann/readLengthCutoff.

642 **Competing Interests**

643 The authors declare no competing interests.

644 **Additional Information**

645 Supplementary information is available for this paper at <https://doi.org/xxxxx>.

646 Correspondence and requests for materials should be addressed to L.D and T.v.d.V.

647 **References (Methods)**

- 648 28. Gansauge, M.-T. & Meyer, M. Single-stranded DNA library preparation for the
649 sequencing of ancient or damaged DNA. *Nat. Protoc.* **8**, 737–748 (2013).
- 650 29. John, J. S. SeqPrep: Tool for stripping adaptors and/or merging paired reads with
651 overlap into single reads. *URL: https://github.com/jstjohn/SeqPrep* (2011).
- 652 30. Schubert, M. *et al.* Improving ancient DNA read mapping against modern reference
653 genomes. *BMC Genomics* **13**, 178 (2012).
- 654 31. Li, H. Aligning sequence reads, clone sequences and assembly contigs with BWA-MEM.
655 *arXiv [q-bio.GN]* (2013).
- 656 32. Feuerborn, T. R. *et al.* Competitive mapping allows for the identification and exclusion of

657 human DNA contamination in ancient faunal genomic datasets. *BMC Genomics* **21**, 844
658 (2020). <https://doi.org/10.1186/s12864-020-07229-y>

659 33. Li, H. *et al.* The Sequence Alignment/Map format and SAMtools. *Bioinformatics* **25**,
660 2078–2079 (2009).

661 34. Jónsson, H., Ginolhac, A., Schubert, M., Johnson, P. L. F. & Orlando, L. mapDamage2.0:
662 fast approximate Bayesian estimates of ancient DNA damage parameters. *Bioinformatics*
663 **29**, 1682–1684 (2013).

664 35. Skoglund, P. *et al.* Separating endogenous ancient DNA from modern day
665 contamination in a Siberian Neandertal. *Proc. Natl. Acad. Sci. U. S. A.* **111**, 2229–2234
666 (2014).

667 36. Korneliussen, T. S., Albrechtsen, A. & Nielsen, R. ANGSD: Analysis of Next Generation
668 Sequencing Data. *BMC Bioinformatics* **15**, 356 (2014).

669 37. Smit, A. F. A., Hubley, R. & Green, P. RepeatMasker Open-4.0. 2013--2015. (2015).

670 38. Green, R. E. *et al.* A complete Neandertal mitochondrial genome sequence determined
671 by high-throughput sequencing. *Cell* **134**, 416–426 (2008).

672 39. Edgar, R. C. MUSCLE: multiple sequence alignment with high accuracy and high
673 throughput. *Nucleic Acids Res.* **32**, 1792–1797 (2004).

674 40. Meyer, M. *et al.* Palaeogenomes of Eurasian straight-tusked elephants challenge the
675 current view of elephant evolution. *Elife* **6**, (2017).

676 41. Yang, Z. Maximum likelihood phylogenetic estimation from DNA sequences with
677 variable rates over sites: approximate methods. *J. Mol. Evol.* **39**, 306–314 (1994).

678 42. Darriba, D., Taboada, G. L., Doallo, R. & Posada, D. jModelTest 2: more models, new
679 heuristics and parallel computing. *Nat. Methods* **9**, 772 (2012).

680 43. Suchard, M. A. *et al.* Bayesian phylogenetic and phylodynamic data integration using
681 BEAST 1.10. *Virus Evol* **4**, vey016 (2018).

682 44. Gill, M. S. *et al.* Improving Bayesian population dynamics inference: a coalescent-based
683 model for multiple loci. *Mol. Biol. Evol.* **30**, 713–724 (2013).

684 45. Lefort, V., Desper, R. & Gascuel, O. FastME 2.0: A Comprehensive, Accurate, and Fast
685 Distance-Based Phylogeny Inference Program. *Mol. Biol. Evol.* **32**, 2798–2800 (2015).

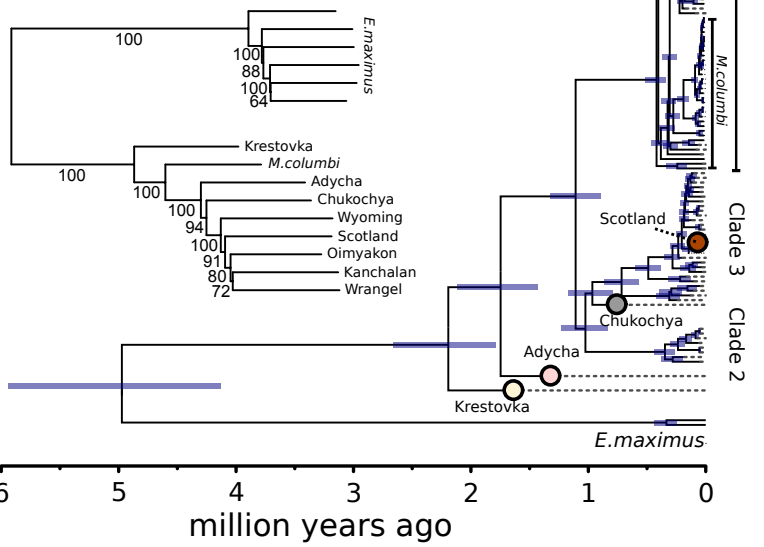
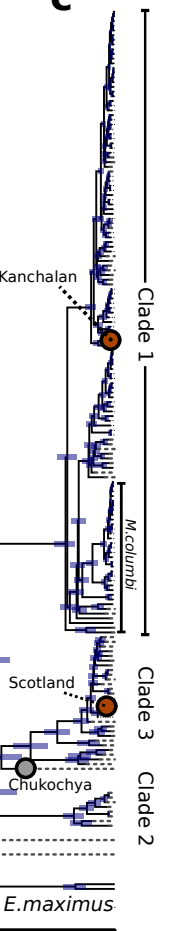
686 46. Liu, L. *et al.* Genomic analysis on pygmy hog reveals extensive interbreeding during wild
687 boar expansion. *Nat. Commun.* **10**, 1992 (2019).

688 47. Frith, M. C., Hamada, M. & Horton, P. Parameters for accurate genome alignment. *BMC*
689 *Bioinformatics* **11**, 80 (2010).

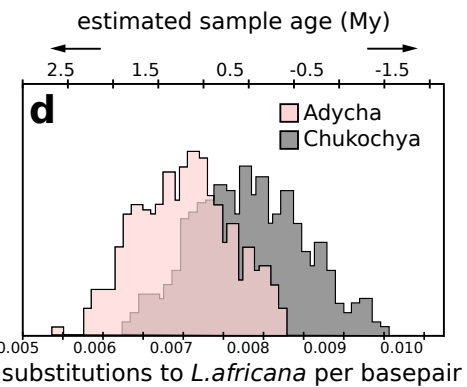
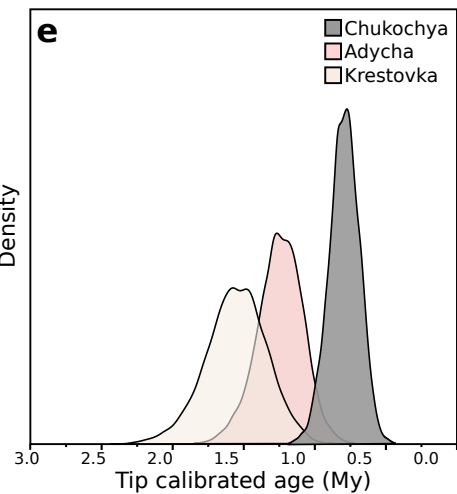
690 48. McLaren, W. *et al.* The Ensembl Variant Effect Predictor. *Genome Biol.* **17**, 122 (2016).

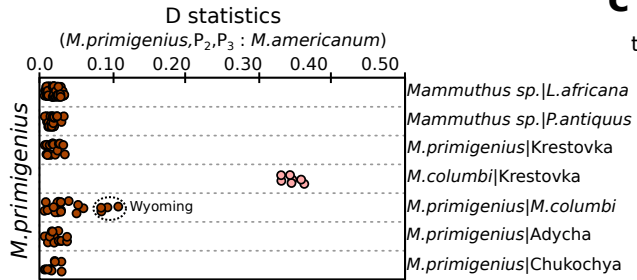
691 49. Eden, E., Navon, R., Steinfeld, I., Lipson, D. & Yakhini, Z. GOrilla: a tool for discovery and
692 visualization of enriched GO terms in ranked gene lists. *BMC Bioinformatics* **10**, 48
693 (2009).

694 50. Yang, Z. PAML 4: phylogenetic analysis by maximum likelihood. *Mol. Biol. Evol.* **24**,
695 1586–1591 (2007).

a**b****c**

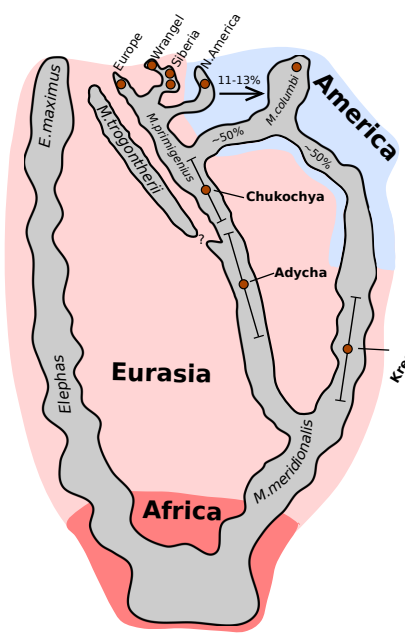
estimated sample age (My)

d**e**

a**c**

genetic
timescale

0.5Ma
1.0Ma
1.5Ma
2.0Ma

**b**